

# ERGONOMICS OF DIRECT-DRIVE RECUMBENT BICYCLES

Jeremy M. Garnet  
Ottawa, ON, Canada

**Abstract** — The direct-drive recumbent bicycle has the crank axle concentric with the front wheel, and a planetary gear front hub. This design offers the advantage of simplicity, good weight distribution and a large load capacity—but has the disadvantage of pedal force feedback to the handlebars due to the fork mounting of the pedals, and excessive front assembly mass due to the weight of the rider's feet on the fork-mounted pedals. Kretschmer (2000) suggests a shallow head angle to reduce the force feedback, and a steering centering spring to improve the handling. This present paper explores the force feedback question further by using pedal loading data available in the literature to determine the force feedback as a function of head angle. A handling analysis is used to determine the correct amount of trail required for the shallower head angle, and a method of calculating the centering spring constant required to counteract the excessive front assembly mass is presented. A variable-geometry bike is employed to give a qualitative, real-life assessment of the results, and to explore the human-factor issues unseen in the equations. The results indicate that the pedal forces which act outside of the plane of rotation of the cranks contribute significantly to reducing pedal force feedback. Test rides on the variable geometry bike show that the head angle should not be inclined below 56 degrees to the horizontal. Other design details, such as handlebar configuration, fork design, and seat height are also discussed, and a final design configuration is presented.

## INTRODUCTION

### The direct drive recumbent bike

The direct-drive recumbent bicycle has the crank axle mounted on the front fork, concentric with the front wheel axis. Gearing is provided by a transmission in the front hub, preferably of a planetary design. Figure 1 illustrates the basic layout of the author's direct drive recumbent.

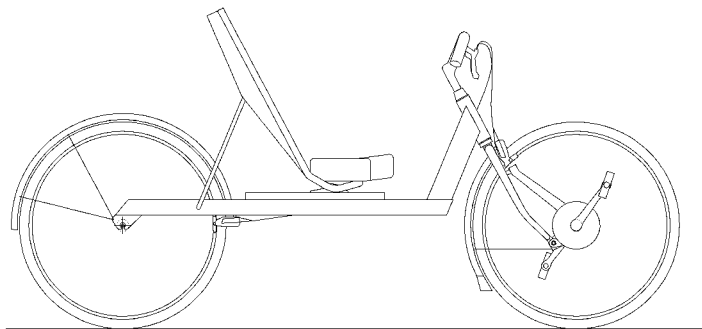


Figure 1: A direct-drive recumbent bicycle

This configuration results in a very simple bicycle with no chain, and it allows a full-size front wheel to be positioned for ideal weight distribution and braking stability. The result is improved

low speed balancing, a smoother ride, lower rolling resistance, and more effective braking. In addition, this can all be achieved with a user-friendly seat height and low bottom bracket, making the design well suited for in-town riding. The cargo carrying capacity of the direct drive recumbent is impressive due to the amount of space made available under the seat by the long wheelbase and absence of chain. Advantageously, the weight of the cargo is centrally located and low down, not disturbing the handling characteristics as much as a rear pannier or rack, for example.

## **A brief history**

The earliest bikes were directly driven and front wheel drive. The ordinary, or high-wheeler is an example. As early as 1892, a planetary gear hub and a smaller wheel were available to replace the huge front wheel—but this design was largely overshadowed by the enormous popularity of the “safety” rear wheel drive chain driven bike. The idea of combining direct front wheel drive with a recumbent riding position dates back to 1893 where a cartoon depicts a rider on what appears to be a directly driven recumbent machine<sup>1</sup>. This seems to have been no more than a humorous suggestion, as it was many decades before the design was explored again.

It was not until the bicycle design renewal in the 1970s that the idea of a direct-drive recumbent was seriously explored. During this period, Thomas<sup>2</sup> introduced a front-wheel-drive recumbent with a crank axle concentric with the front wheel as a convenient way of combining hand and foot power for increased acceleration. This bike, however, was chain driven, with an intermediate shaft mounted above the front wheel.

More recently Kretschmer (2000) proposed and designed a direct-drive recumbent with a planetary gear hub for which he has German patents<sup>3</sup>. Stegmann (2002) has also proposed a direct drive design, which takes full advantage of the cargo-carrying capacity available. The author (Garnet (2003)) has designed and built a direct-drive recumbent using a modification of a Schlumpf Speed-Drive® unit.

## **Scope of the research**

The scope of this paper is divided into three parts: a) pedal force feedback analysis, b) handling analysis, and c) experimental analysis. All three of these analyses are used to establish a recommended geometry for a direct-drive recumbent bike.

## **Pedal force feedback analysis**

Since the pedals are fork mounted<sup>4</sup> rather than frame mounted, the rider’s pedaling force generates an alternating steering torque. The cyclist must resist this steering torque through the handlebars in order to ride efficiently and in a straight line. From the author’s own cycling experience, this torque is not as strong as originally expected, and, with experience, the bike can be tracked accurately without difficulty. Also, the involvement of the arms and upper body in the pedaling process is not unpleasant but brings a certain athletic appeal to the riding. However, on long rides and under heavy acceleration it can be tiring to the arms, hands and upper back. A reduction in this pedal force feedback<sup>5</sup> would be a welcome improvement to the

---

<sup>1</sup> See Fehlau (2003), p9.

<sup>2</sup> See summary of direct-drive recumbent history in Stegmann (2002).

<sup>3</sup> DE 19736266 and DE 19824745.

<sup>4</sup> Fork mounted pedals are also known as ‘moving bottom bracket’, ‘moving BB’, or simply ‘MBB’.

<sup>5</sup> The pedal force feedback is also known as pedal/steering interference (PSI) and is present in other bicycles with moving bottom brackets. A discussion of PSI in other bikes is given in the results section

bike, and would result in a design that was more user-friendly for new riders.

Kretschmer (2000) suggests a shallow head angle to reduce the pedal force feedback. The shallow inclination aligns the head axis more closely with the direction of the applied pedal force, reducing the resulting torque about the steering axis. However, a shallow head angle can have an adverse effect on handling. Therefore it would be useful to know exactly how the alternating steering torque varies with head angle in order to find the best compromise between low pedal force feedback and user-friendly handling. Therefore the scope of the pedal force feedback analysis is to determine the pedal force feedback as a function of head angle.

### **Handling analysis**

In a direct-drive recumbent, the mass of the front assembly is much larger than in a regular bike because it includes the mass of the rider's feet and the portion of the rider's legs which rotates with the steering. This results in a front assembly mass in the region of 15 to 20 kilograms rather than the typical 2 to 4 kilograms. The centre of this mass is located further from the steering axis than on a regular bicycle, due to the increased fork offset that arises from the reduced head angle.

The greater mass and distance combine to increase the torque that is generated around the steering axis when the bicycle is leaned into a turn, or when the steering is turned off-center. This results in over-control, with more steering response than necessary for stable hands-free riding. To address this issue, a direct-drive recumbent requires a different frame and fork geometry. Kretschmer (2000) suggests 2-3 cm of trail (compared about 5-6 cm in conventional bikes), and also recommends a centering spring for the steering.

The scope of the handling analysis is to determine the trail and centering spring constant that is needed to address the excessive front assembly mass and inclined head angle.

### **Experimental analysis**

In a study of ergonomics, the final word should go to the actual experience of the rider. Therefore the results of the above calculations are evaluated experimentally, by means of a direct drive recumbent bike having a variable geometry frame. This is a qualitative assessment rather than quantitative; the purpose is to find out how it feels to ride a direct drive recumbent of a given geometry, and to determine an optimum geometry for user comfort.

## **METHODS**

### **A. PEDAL FORCE FEEDBACK**

The pedal force feedback is evaluated analytically using pedal force data available in the literature. For the force feedback evaluation, the steering is assumed to be in the straight ahead position (on-centre) and the frame of the bike vertical.

### **Choice of input data**

---

and also in Openbike (2008).

There are many good experimental results now available on pedal forces<sup>6</sup>. Hull and Davis (1981) and Davis and Hull (1981) have researched rider pedal forces, including the forces generated outside of the plane of rotation of the pedal cranks. They discovered that these out-of-plane forces are significant, particularly the lateral force generated in the outward direction. For the direct drive recumbent case this is an important factor, due to the significant lever arm present from the large fork offset associated with shallow head angles. This fork offset can be larger than the lateral offset of the pedal from the centerline of the bike. Hull and Davis (1981) present their experimental method along with a typical test result, and Davis and Hull (1981) present some further test runs for different riders, focusing on pedal securing methods, rider power levels, and the effect of rider training on pedaling efficiency. To give some diversity of riders and power levels, five data sets are taken as input data: the test run given in figures 9 and 10 of Hull and Davis (1981), and four test runs given in figures 6-9 in Davis and Hull (1981). In all these test runs, the riders wore toe-clips and cleats (note that in what follows “Hull and Davis” is used to denote the combined work of Hull and Davis (1981) and Davis and Hull (1981)).

### Translating to recumbent position

The data of Hull and Davis was taken from an upright test bike, rather than a recumbent. Since the gravitational component of the pedal force acts in the same direction and magnitude on both pedals, the net effect of gravity on the pedal-induced steering torque is zero. Therefore the results of Hull and Davis are also applicable to the recumbent position, provided that the crank angle is referenced to the same leg position. This is done by referencing the crank position to a line joining the hip pivot of the rider and the bottom bracket axis (see figure 2). Hull and Davis give no indication of the hip pivot of their rider. For an upright bike, however, it is reasonable to assume that the hip pivot is in line with the axis of the seat tube of the bike, so the seat tube angle was taken as the reference angle. The seat tube angle of the test bike used in Hull and Davis was not specified, so a typical seat tube angle of 73 degrees to the horizontal is assumed.

The hip pivot for the direct drive bike is measured from an actual rider. The angle of a line from the hip pivot to the bottom bracket axis (front wheel axis) is then determined from the geometry of the bike. The difference between this angle and the 73 degree reference angle is defined as the recumbent angle:

$$\theta_R = 73^\circ - \text{Arcsin} \frac{H_{hp} - H_{bb}}{L_R} \quad (1)$$

where,

$\theta_R$  = recumbent angle

$H_{hp}$  = height of the hip flexure point of the rider

$H_{bb}$  = bottom bracket height (equal to front wheel radius)

$L_R$  = distance from hip flexure point to bottom bracket

---

<sup>6</sup> For a discussion of available pedal force data see Wilson (2004), pp. 79-83.

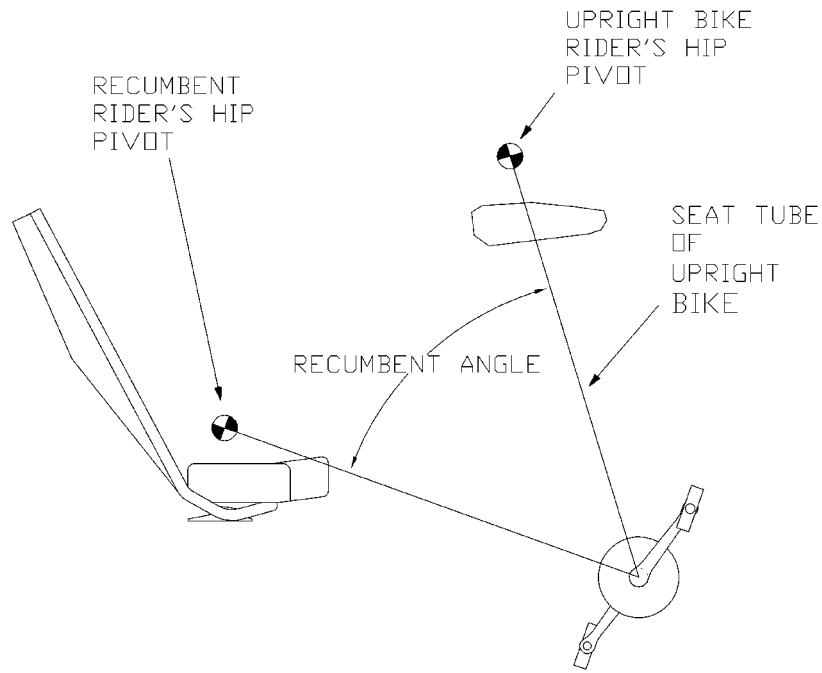


Figure 2: Defining the recumbent angle

### Referencing to the head axis

The recumbent angle and the head angle are used to reference the pedal and crank angles given in Hull and Davis to the head axis (as shown in figure 3). This gives:

$$\theta_{P_H} = \theta_R - \theta_{P_{HORIZ}} + \theta_H \quad (2)$$

where,

$\theta_{P_H}$  = pedal angle relative to the head axis

$\theta_{P_{HORIZ}}$  = pedal angle relative to the horizontal given in Hull and Davis

$\theta_H$  = head angle ( relative to the horizontal)

and,

$$\theta_{C_H} = \theta_R - \theta_{C_{VERT}} + 90^\circ + \theta_H \quad (3)$$

where,

$\theta_{C_H}$  = crank angle relative to the head axis

$\theta_{C_{VERT}}$  = crank angle relative to the vertical given in Hull and Davis

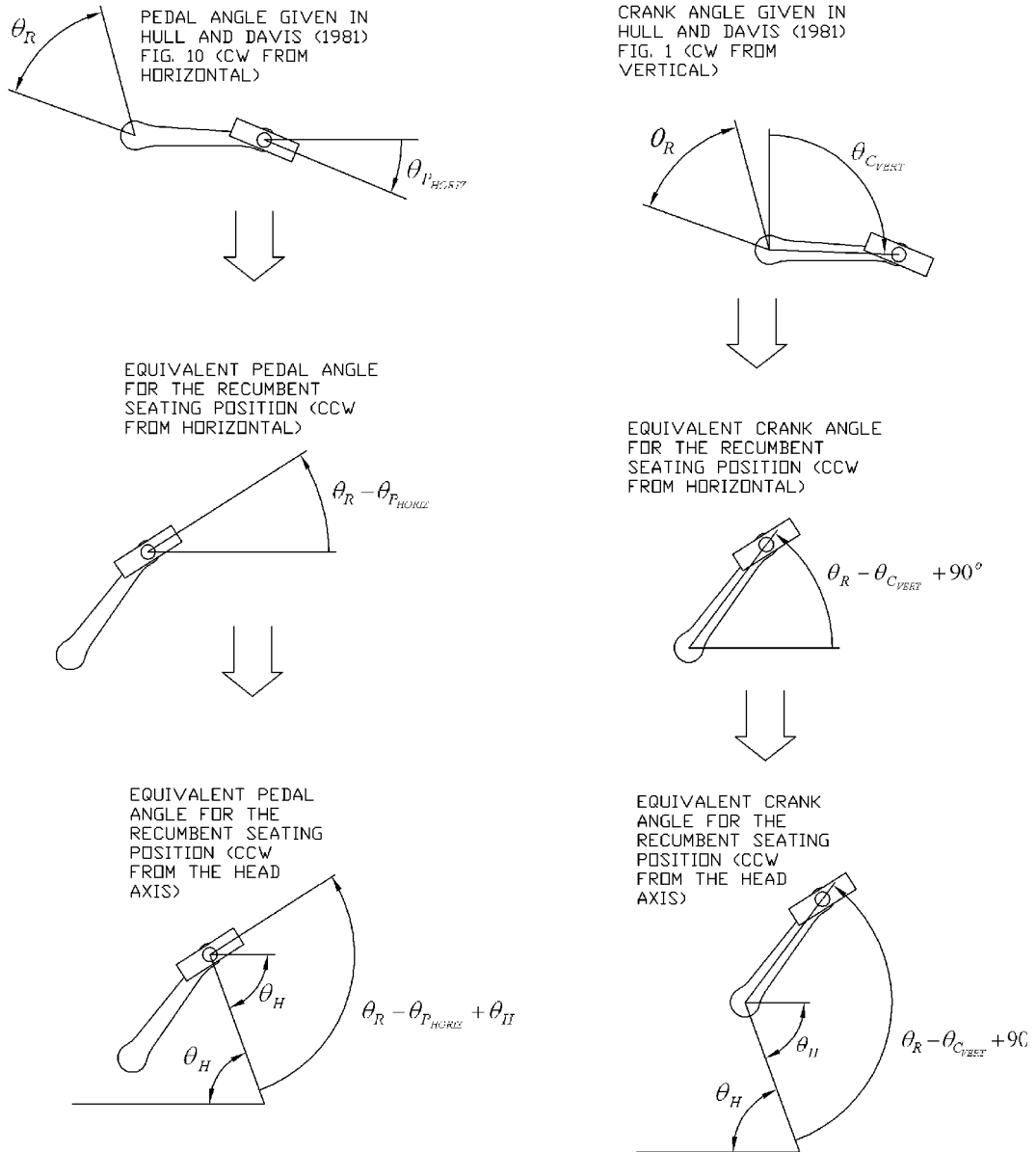


Figure 3: Referencing pedal and crank positions to the steering axis

**Determining the torque contribution of each of the 6-axes:**

Referring to figure 4, the steering torque contribution of each of the pedal forces and moments is calculated as follows:

$$M_{F_X} = \frac{Q}{2} F_X \sin \theta_{P_H} \quad (4)$$

$$M_{F_Y} = F_Y \left( d_F + L_C \sin \theta_{C_H} \right) \quad (5)$$

$$M_{F_Z} = \frac{Q}{2} F_Z \sin \theta_{P_H} \quad (6)$$

$$M_{M_X} = M_X \sin \theta_{P_H} \quad (7)$$

$$M_{M_Y} \equiv 0 \quad (\text{acts in a plane parallel to the steering axis}) \quad (8)$$

$$M_{M_Z} = M_Z \sin \theta_{P_H} \quad (9)$$

where,

$F_X, F_Y, F_Z$  = pedal force in the x, y, and z direction, respectively, from Hull and Davis

$M_X, M_Y, M_Z$  = pedal moment in the x, y, and z-direction, respectively, from Hull and Davis

$M_{F_X}, M_{F_Y}, M_{F_Z}$  = steering moment due to pedal force in the x, y, and z-direction, respectively

$M_{M_X}, M_{M_Y}, M_{M_Z}$  = steering moment due to pedal moment in the x, y, and z-direction, respectively

$Q$  = tread (lateral distance from centre-of-pedal to centre-of-pedal)

$L_C$  = crank length

$d_F$  = fork offset =  $(r_F - T \tan \theta_H) \cos \theta_H$

$r_F$  = front wheel radius

$T$  = trail of the front wheel

### Determining the total net torque about the head axis

The total torque about the head axis is the sum of contributions of each of the three forces and moments. At each crank position, the total net torque will be the total torque due to the right pedal minus the total torque due to the left pedal calculated at a crank position 180 degrees opposed. This gives:

$$M_{TOTAL, NET}_{\theta_c} = \left\{ \sum_{i=x,y,z} M_{F_i} + M_{M_i} \right\}_{\theta_c} - \left\{ \sum_{i=x,y,z} M_{F_i} + M_{M_i} \right\}_{\theta_c - 180^\circ} \quad (10)$$

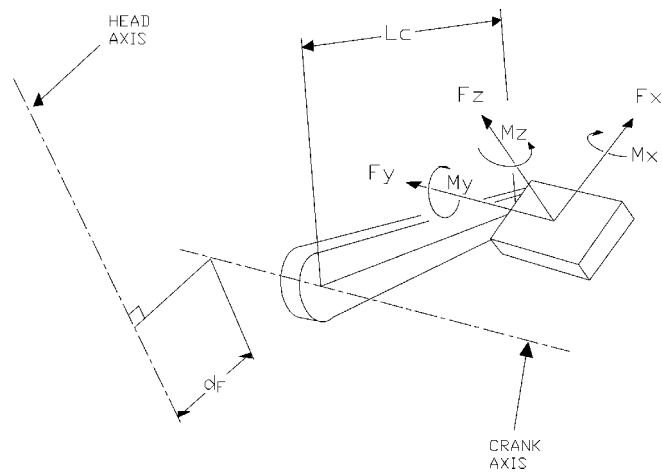


Figure 4: Pedal load components of Hull and Davis (1981) shown relative to the head axis

### Determining the resulting force restrained by the hands of the rider

The force that the rider must exert to restrain the net torque depends not only on the torque given in equation (10), but also on the handlebar position.

To compare the effectiveness of different handlebar positions, one must evaluate both the direction of the restraint of the arms with respect to the steering axis and the anatomical efficiency of the arms in the restraining position.

Three handlebar positions are commonly used in recumbent bicycles: above-seat, below-seat, and hamster position. Figure 5 depicts a direct-drive recumbent with the above-seat handlebar position. Figures 6 and 7 illustrate the below-seat and hamster handlebar positions, respectively.

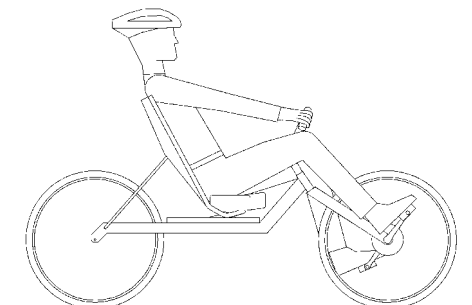


Figure 5: Above-seat handlebar position



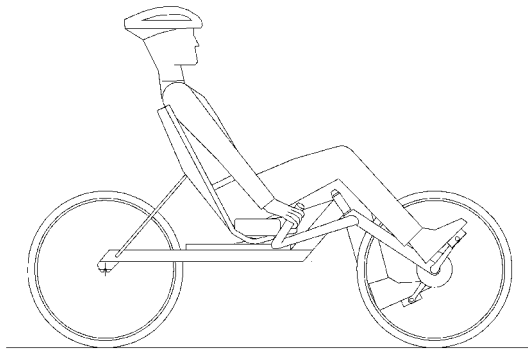


Figure 6: Below-seat handlebar position

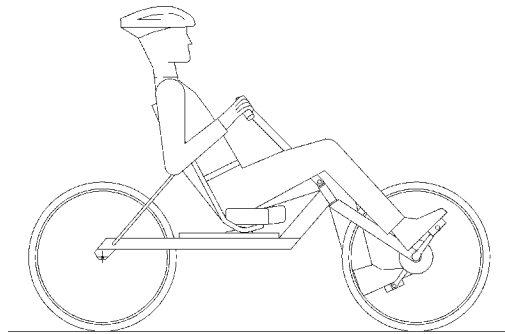


Figure 7: Hamster handlebar position

The above-seat, arms outstretched position allows the arms to be “locked” in the outstretched position, forming a mechanical brace between the seat back and the handlebar grips. This reduces the contribution required of the muscles in the arms, resulting in lower rider fatigue. This can be demonstrated by the ease with which a person can hold themselves at the top of a push-up exercise, compared to the difficulty of holding a position halfway up where the elbows form an angle. The leverage in the locked axial direction of the arms with respect to the steering axis is good, but this mechanical advantage diminishes as the steering axis is inclined.

The below-seat position also allows the arms to lock in an outstretched position, but the plane of the outstretched arms is nearly parallel to the steering axis. Therefore the leverage obtained in the axial direction of the arms is poor relative to the steering axis. As a result, the advantage of the mechanical brace of the outstretched arms is lost, and the arms will instead resist the pedal induced torque by exerting a force perpendicular to the axial direction of the arms. This is highly strenuous for the associated muscle groups.

The hamster position lacks the bracing advantage of the outstretched arms, resulting in a greater contribution by the muscle groups in the arms, and correspondingly increased muscular fatigue.

Therefore, of the three possible positions, the above seat outstretched arm position is the superior choice for a direct-drive recumbent. This is also the handlebar position preferred by Stegmann (Stegmann (2002)).

Therefore, the outstretched arm position is judged the best of the three configurations, and it is the handlebar position adopted in the analysis.

The force restrained by the hands of the rider, acting in line with the rider's arms, is thus:

$$F_H = \frac{M_{TOTAL, NET_{\theta_c}}}{W \sin(\theta_H - \theta_A)} \quad (11)$$

where,

$F_H$  = force that each hand must exert to restrain the torque about the head axis

$\theta_A$  = angle of the plane of the outstretched arms (relative to the horizontal, hands below shoulders)

$W$  = handlebar width (between handlebar grip centres)

The plane of the outstretched arms is the plane passing through the shoulder joints of the rider and the centre of each handlebar grip.

## B. HANDLING ANALYSIS

The handling of a bicycle arises from a complex interaction of gravitational, inertial and gyroscopic forces. For a thorough analysis of bicycle handling and stability, with the governing equations, see Wilson (2004) or Papadopoulos (1987).

The handling analysis considered here is simplified by considering low speed handling only, and by equating parameters to a reference bike, rather than calculating them on absolute terms. Both these simplifications are consistent with the objective of user-friendliness, since it is at low speed that the all-important first impression of handling is experienced, and setting characteristics to a known type of bike ensures familiarity for the new user.

For a given head angle, the front wheel trail and the steering centering spring will determine how a direct-drive recumbent handles. Therefore these two parameters are derived as a function of head angle. At low speed, gyroscopic forces are low, and a static analysis of the applied gravitational forces on the steering can be used to set the front wheel trail and design an effective centering spring. Papadopoulos (1987) presents a simplification based on a static analysis, and the approach that follows is similar to this.

When a stationary bike is held vertically and the steering is turned from the centre, a torque is generated about the head axis (figure 8). A steering torque is also generated when the bike is leaned to one side with the steering held on-centre (figure 9). These two effects, which can be investigated separately, are known as steering-induced torque and lean-induced torque, respectively. Steering induced torque is also commonly referred to as "fork flop".

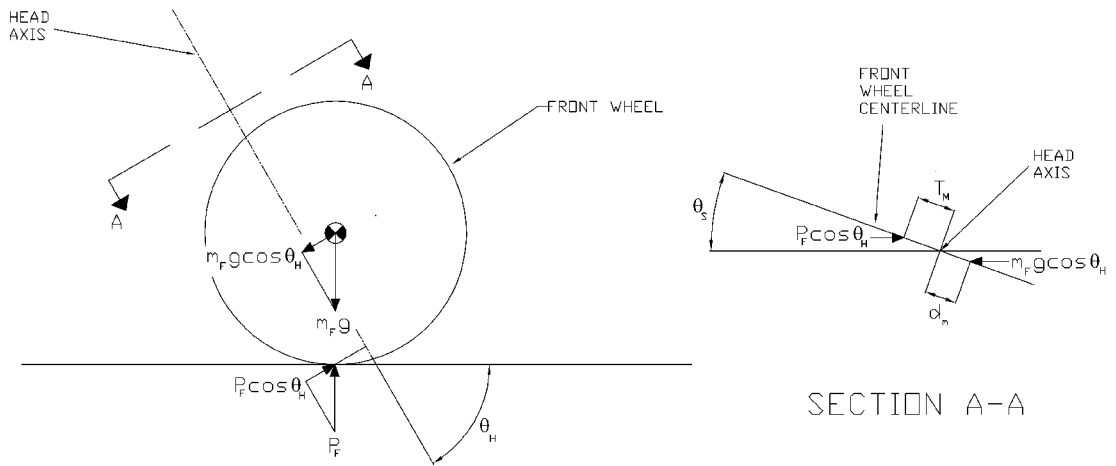


Figure 8: Steering-induced torque

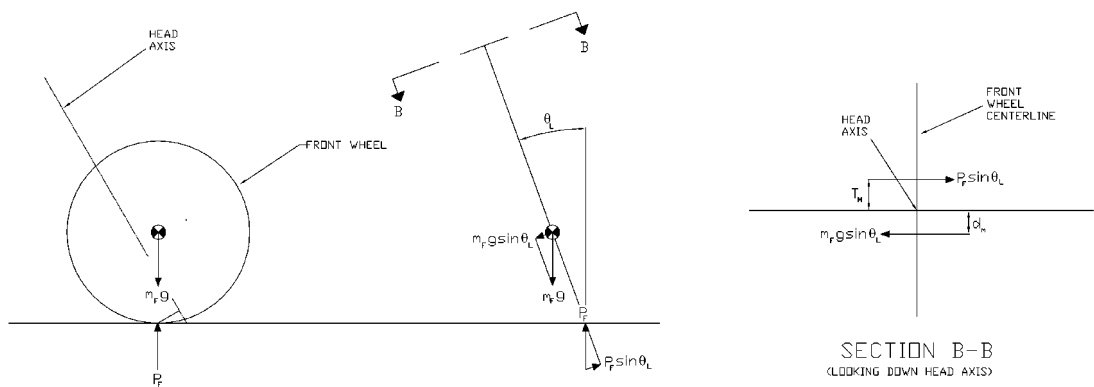


Figure 9: Lean-induced torque

The steering-induced torque and lean-induced torque result from two applied gravitational forces: the force of the ground on the front wheel and the force due to the offset mass of the front assembly. “Offset mass of the front assembly” means that the centre of gravity of the front assembly (i.e. all the parts that swings with the steering) is offset from the head axis.

Referring to figures 8 and 9, this yields four equations:

$$M_{\theta_S, P_F} = P_F T_M \cos \theta_H \sin \theta_S \quad (12)$$

$$M_{\theta_S, m_F} = m_F g d_m \cos \theta_H \sin \theta_S \quad (13)$$

$$M_{\theta_L, P_F} = P_F T_M \sin \theta_L \quad (14)$$

$$M_{\theta_L, m_F} = m_F g d_m \sin \theta_L \quad (15)$$

where,

$M_{\theta_S, P_F}$  = steering induced torque due to ground force on front wheel

$M_{\theta_S, m_F}$  = steering induced torque due to offset front assembly mass

$M_{\theta_L, P_F}$  = lean induced torque due to ground force on the front wheel

$M_{\theta_L, m_F}$  = lean induced torque due to offset front assembly mass

$P_F$  = ground force on the front wheel

$T_M$  = mechanical trail (trail of front wheel perpendicular to the head axis) =  $T \sin \theta_H$

$\theta_S$  = steering angle from centre

$\theta_L$  = lean angle from equilibrium

$m_F$  = mass of the front assembly

$g$  = gravitational acceleration

$d_m$  = offset of front assembly centre of mass from head axis

The design challenge is to reduce the steering-induced torque and lean-induced torque to a level that is similar to that of an upright bike. There are several ways of achieving this reduction.

### **The question of negative trail**

Papadopoulos (1987) suggests that a bicycle with a large offset front assembly mass may benefit from some negative trail. With negative trail, the ground force on the front wheel produces a torque in a direction opposite to the torque coming from the offset front assembly mass. The correct amount of negative trail can therefore be used to counteract the effect of excessive front assembly mass, leading to a manageable torque for good handling. This is very appealing theoretically because the effect is balanced proportionally to the lean angle, whereas a centering spring can only be made proportional to the steering angle.

The difficulty with this approach stems from the exclusion of all forces except gravity. There are other forces which act laterally on the front wheel besides lean-induced gravity forces. Lateral forces also act on the front wheel due to uneven pavement, bumps and ridges. Since the resistance to these forces is inertial (and, at higher speed, also gyroscopic), the much larger moment of inertia of the rear assembly predominates, forcing the front assembly to rotate in the same direction as the applied force and thus in a direction opposite to restoring balance. This produces a bike that may be quite stable on a smooth flat surface, but very jittery and unsettling

to ride on a rough surface.

Experiments with a variable geometry bike confirm this (the variable geometry bike is described in the next section). A negative trail value that has this desired counterbalancing effect is about 60mm for a 56 degree head angle. The steering is well constrained on smooth turns, but the overall response of the bike is highly unfamiliar, particularly at low speed and on uneven surfaces. Therefore, in spite of the theoretical advantages of negative trail in controlling excessive front assembly mass, it is rejected because it lacks overall user-friendliness and stability.

### **The question of a counter-balance mass**

Ruling out negative trail, the only other way of balancing the offset front assembly mass proportionally with the lean angle is to add a counter-balance mass to the front assembly. This mass would have to be considerable, however, since the offset front assembly mass is large. Extra mass is of course the last thing wanted on a bike, and a counter-balance mass would also increase the radius of gyration of the front assembly, leading to unusual handling. Therefore this idea is rejected also.

### **Lean-induced torque relative to steering-induced torque**

Clearly there are difficulties in designing a means to resist excessive lean-induced torque. Therefore the question arises as to whether, in everyday riding, lean-induced torque is significant compared to the steering-induced torque. At shallow head angles the  $\cos\theta_h$  term in equations (12) and (13) becomes significant (equal to 0.64 for 50 deg, for example), so the influence of these two steering-induced equations approaches that of the corresponding lean-induced equations (14) and (15). As a result, the influence of the lean-induced torque relative to the steering-induced torque becomes essentially a question of typical lean angles relative to typical steering angles.

The lean angle used in the equations is the lean angle relative to the vertical position when the bike is steered straight. It represents the lean angle relative to the equilibrium lean of the frame. A large lean angle from equilibrium is unlikely in everyday riding since it would mean that the rider was well on the way to capsizing. The rider unconsciously does not allow large lean angles from equilibrium to develop. Steering angles, in contrast, can be relatively large during normal riding, particularly at low speed.

Therefore it is judged acceptable to neglect the lean-induced steering torque as a simplification. Addressing the steering-induced effects alone will at least control the excessive fork flop, and fork flop is the most common complaint about bikes with shallow head angles.

### **Determining trail**

The trail is determined by setting the steering-induced torque due to ground force (equation 12) of a new bike to that of a reference bike. Therefore, for a given steering angle:

$$\left[ P_F T_M \cos \theta_H \right]_{NEW} = \left[ P_F T_M \cos \theta_H \right]_{REF} \quad (16)$$

This gives,

$$T_{NEW} = T_{REF} \frac{\left[ P_F \sin \theta_H \cos \theta_H \right]_{REF}}{\left[ P_F \sin \theta_H \cos \theta_H \right]_{NEW}} \quad (17)$$

Or, assuming the two bike/rider combinations are of a similar weight:

$$T_{NEW} = T_{REF} \frac{\left[ F_F \sin \theta_H \cos \theta_H \right]_{REF}}{\left[ F_F \sin \theta_H \cos \theta_H \right]_{NEW}} \quad (18)$$

Where,

$F_F$  = fraction of total weight that is on the front wheel

### Determining the centering spring characteristic

Since the trail is calculated so as to eliminate the excessive steering-induced torque due to the ground force, the centering spring need only address the excessive steering-induced torque due to the excessive front assembly mass. Equating new and reference values of equation (13) yields, with a centering spring added for the new bike:

$$g \sin \theta_S \left[ m_F d_m \cos \theta_H \right]_{NEW} - M_{SPRING} = g \sin \theta_S \left[ m_F d_m \cos \theta_H \right]_{REF} \quad (19)$$

Thus the moment the centering spring must develop is,

$$M_{SPRING} = g \sin \theta_S \left[ \left( m_F d_m \cos \theta_H \right)_{NEW} - \left( m_F d_m \cos \theta_H \right)_{REF} \right] \quad (20)$$

Since typical steering angles are less than about 30 degrees,

$$\sin \theta_S \approx \theta_S \quad (\text{where } \theta_S \text{ is in radians}) \quad (21)$$

Therefore the required torsion spring rate (per radian) is simply:

$$K_{SPRING} = g \left[ \left( m_F d_m \cos \theta_H \right)_{NEW} - \left( m_F d_m \cos \theta_H \right)_{REF} \right] \quad (22)$$

If the offset of the front assembly centre of mass is assumed to be the same as the fork offset (this is a reasonable assumption), then,

$$K_{SPRING} = g \left[ \left( m_F d_F \cos \theta_H \right)_{NEW} - \left( m_F d_F \cos \theta_H \right)_{REF} \right] \quad (23)$$

Thus a centering spring characteristic for a new bike can be determined based on the front assembly mass, head angle, and fork offset of the new bike and the reference bike.

### C. EXPERIMENTAL ANALYSIS

The purpose of the experimental part of this study is to assess the calculated results qualitatively. To do this a variable geometry bike was constructed to test the head angles with the corresponding trail values and spring constants. Figure 10 depicts the variable geometry bike. The bike employs the wheels, seat, handlebars, brakes, and transmission of the author's bike of figure 1.

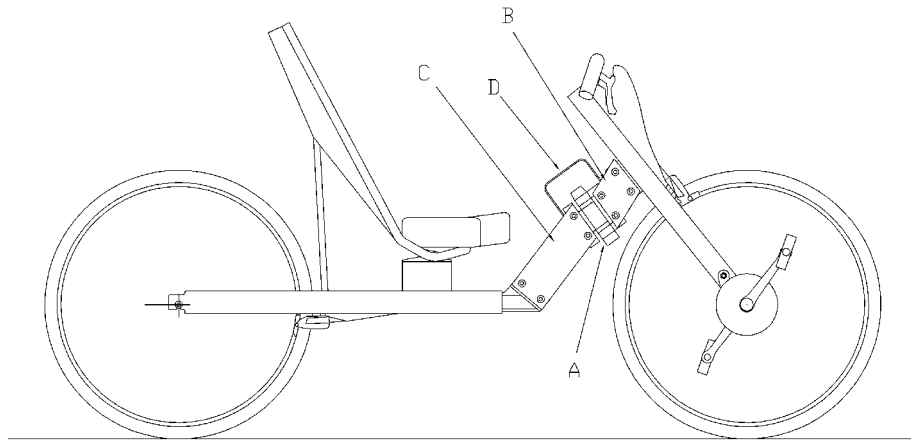


Figure 10: Variable geometry test bike

The frame of the variable geometry bike is constructed so that changes in head angle and trail do not affect the positioning of the major frame members, and so that the position of the rider on the bike remains unchanged. This is done by using a headset hinge (A) which can be located in a range of positions on the “down tube” of the frame. The down tube is, in fact, not a tube but rather it is composed of four plates: two upper plates (B) and two lower plates (C) which sandwich the respective hinge flanges. At the opposite ends the lower plates sandwich a flange attached to the main horizontal frame member, and at the upper end the upper plates surround a flange attached to the fork assembly. The plates are accurately machined and held to the flanges by shoulder bolts. Thus by changing the four plates both the head angle and the trail can be changed.

A torsion bar spring (D) is placed between the two top plates and the two bottom plates to act as the centering spring. It is generally hat-shaped, with the vertical parts, which are parallel to the head axis, acting as torsion bars. The active length is thus the sum of the vertical lengths.

## RESULTS

Table 1 lists the input values for the direct-drive recumbent bike. These values are based on the variable geometry frame and may, of course, differ in a possible future production bike. For example, the front wheel weight fraction is taken as 0.5 (based on the variable geometry frame's actual reading of 49%), but it may be more or less than this depending on the wheelbase. Also the mass of the front assembly will probably be less than the measured 19.5 kg in a production bike, since the fork will be better optimized for lightness (the variable geometry frame is constructed for dimensional accuracy rather than low weight). It is unlikely, however, that the front assembly mass will ever be much less than 15kg for an adult rider since the weight of the rider's feet resting on the pedal is included. Measurements were taken from an actual rider, (male, 1.83m tall, 89 kg) so these will also vary.

Table 1: Input values for direct-drive recumbent bike

Head angle (from horizontal)	variable	
Radius of front wheel	348 mm	13.7 in
Fraction of weight on front wheel (bike and rider)	0.5	
Tread (lateral distance between pedal centers)	297 mm	11.7 in
Handlebar grip width (between grip centers)	465 mm	18.3 in
Seat height (defined as 76 mm (3 in) below hip pivot of rider)	554 mm	21.8 in
Distance from hip pivot to bottom bracket	841 mm	33.1 in
Crank length	170 mm	6.69 in
Plane of restraint of rider's arms (above horizontal)	0.244 radians	14 degrees
Mass of the front assembly (including rider's proportion)	19.5 kg	43 lbs

Table 2 gives the input value for the reference bike. The reference bike is not one particular bike, but a "generic" upright bike. It represents a typical upright bike to which the user is familiar.

Table 2: Input values for reference upright bike

Head angle (from horizontal)	72 degrees	
Radius of front wheel	348 mm	13.7 in
Fraction of weight on front wheel (bike and rider)	0.4	
Trail	50.8 mm	2.0 in
Seat tube angle (from horizontal)	73 degrees	
Mass of the front assembly	3.64 kg	8.0 lbs

### A. PEDAL FORCE FEEDBACK ANALYSIS

The results presented are the average results based on the five sets of input data of Hull and Davis.



## Steering torque variation with crank position

The pedal force feedback varies as the crank rotates. Figure 11 shows a typical variation with crank position. The head angle is 62 degrees to the horizontal (the same as that of the author's bike - figure 1). Note that the zero degree position is when the right crank is aligned with the head angle, and facing downward and forward (the same zero reference as in figure 3).

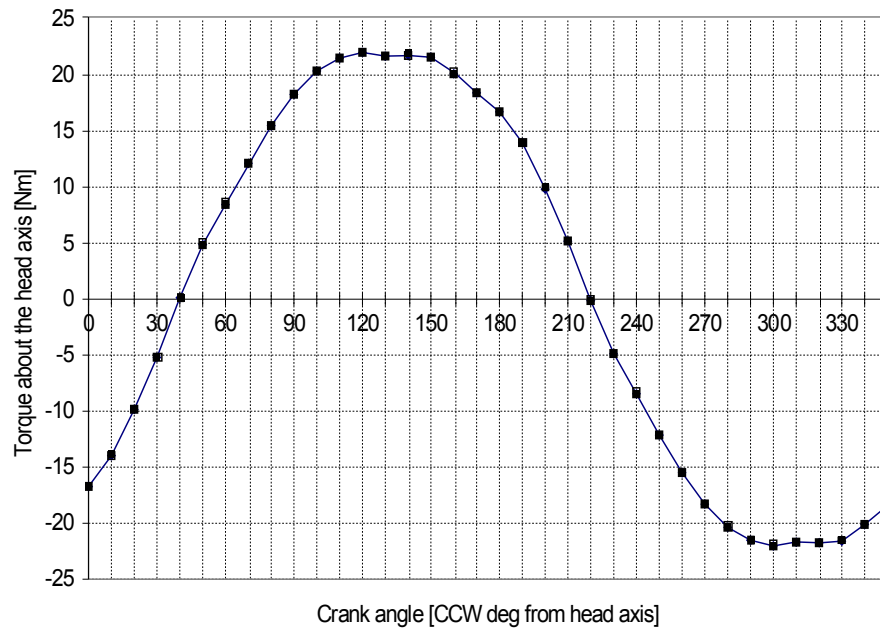


Figure 11: Torque vs. crank angle

Figure 11 indicates that the pedaling torque feedback to the handlebars follows an approximately sinusoidal curve, with a maximum value when the right pedal crank is oriented at about 120 degrees counterclockwise (CCW) from the inclination of the head axis. There is a considerable flat portion of the curve extending from 120 to 150 degrees. Since the head angle in figure 11 is 62 degrees to the horizontal, this range is from 2 to 32 degrees after the top vertical position in the normal clockwise sense of the rotation of the right crank. This makes intuitive sense since, for the low-bottom bracket recumbent position, this crank angle range is close to the peak of the power stroke, yet the applied pedal forces are still considerably inclined relative to the head angle plane, giving good mechanical advantage relative to the steering axis.

## Maximum steering torque due to pedaling

The severity of the pedal force feedback can be expressed as the maximum torque generated about the steering axis for each 360 degree rotation of the cranks. Figure 12 depicts this torque as a function of the head angle, when only the components acting in the plane of rotation of the cranks are included (in-plane only), and when all the components are included (all components). A comparison of the “all components” curve to the “in-plane only” indicates that the out-of-plane forces reduce the pedal force feedback to a remarkable degree (as much as 63%). Also the out-of-plane forces cause the minimum torque to shift to the right (i.e. to a steeper head angle).

The minimum becomes 44 degrees, rather than 28 degrees for the in-plane only case (off the scale of this figure). The result is a steeper slope in the more practical range of head angles (54 to 72 degrees). Thus the out-of-plane forces are of a double benefit to the direct-drive recumbent designer: they reduce the force feedback and increase the effectiveness of reducing the head angle. This out-of-plane effect is predominately due to the outward lateral force which was found by Hull and Davis to be generally in phase with the principal pedal force.

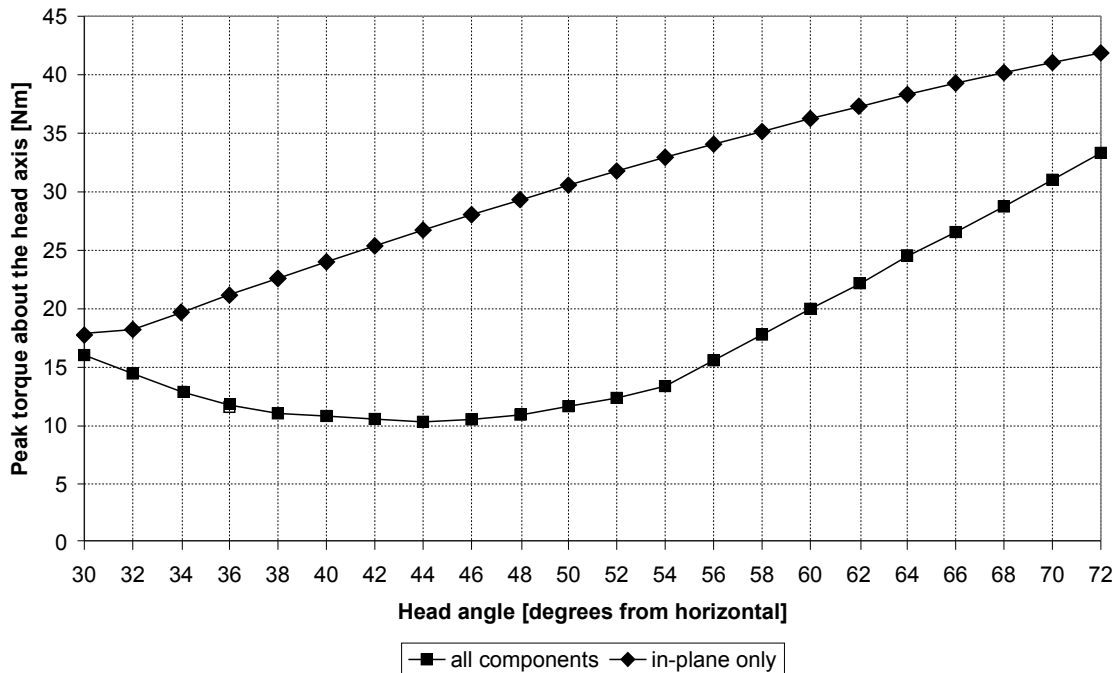


Figure 12: Peak torque vs. head angle

The outward lateral pedal force arises from the direction of the force applied by the rider’s foot to the pedal. The line of this force passes through the center of pressure of the rider’s body on the seat, creating an outward component at the pedals.

Since the data of Hull and Davis was taken from an upright bike, the question arises as to whether the restraint of the rider’s body on a recumbent seat is so different from an upright’s that the lateral pedal forces of Hull and Davis are not applicable to a recumbent. However with the relatively upright seating position of the direct-drive recumbent, much of the rider’s weight will still be centered on the seat cushion. Therefore the outward angle of the load path should be similar to that of an upright bike, and thus the lateral pedal force data of Hull and Davis still applicable.

Figure 13 illustrates the peak torque around the steering axis expressed as a percentage of the peak torque applied to the crank axis. This gives a sense of how much of the torque required for propelling the bike is returned to the handlebars. As shown, shallow head angles can reduce this to a little less than 20 percent.

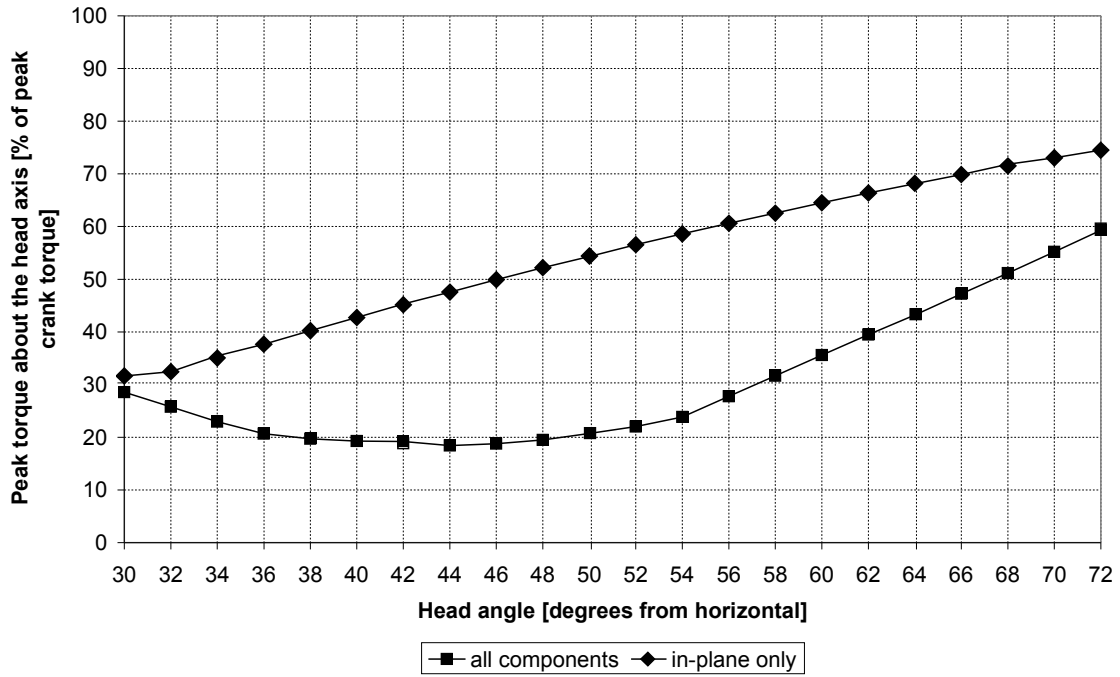


Figure 13: Peak torque as a function of peak pedaling torque

Figure 14 shows the root-mean-square (RMS) torque about the steering axis. This is the square root of the sum of the squares of the steering torque for every 10 degrees of crank rotation over a 360 degree range. Both the “all components” and “in-plane” cases are presented.

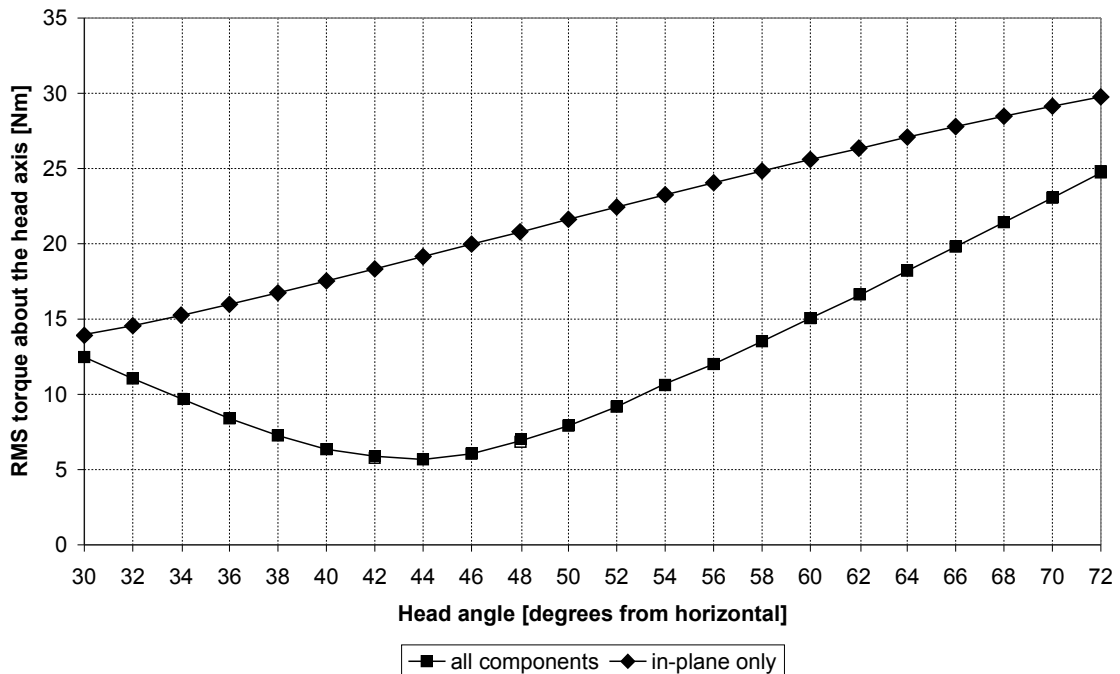


Figure 14: RMS torque vs. head angle

The RMS (root-mean-square) torque about the head axis follows a similar trend to the peak torque, with the minimum remaining at 44 degrees for the “all components” case. The curve is

smoother and there is less of a flat section surrounding the minimum (36 to 54 degrees). The difference between the peak and RMS curves in this section indicates that the torque varies less smoothly with the crank angle in this region. However, while the RMS torque is of theoretical interest, it is the peak torque that is the most relevant to the rider. In fact the RMS result may hide a highly unwanted “spike” in the torque. Therefore a reduction in peak values is judged the best indicator of user-friendliness.

### Peak handlebar restraining force vs. head angle

The force that the rider’s hands will actually have to restrain is dependent on the plane of restraint of the rider’s hands. The resulting peak restraining force required of each hand is given in figure 15 as a function of head angle, for all pedal components and for “in-plane” only. The restraining force component depicted is that which acts in line with rider’s arms.

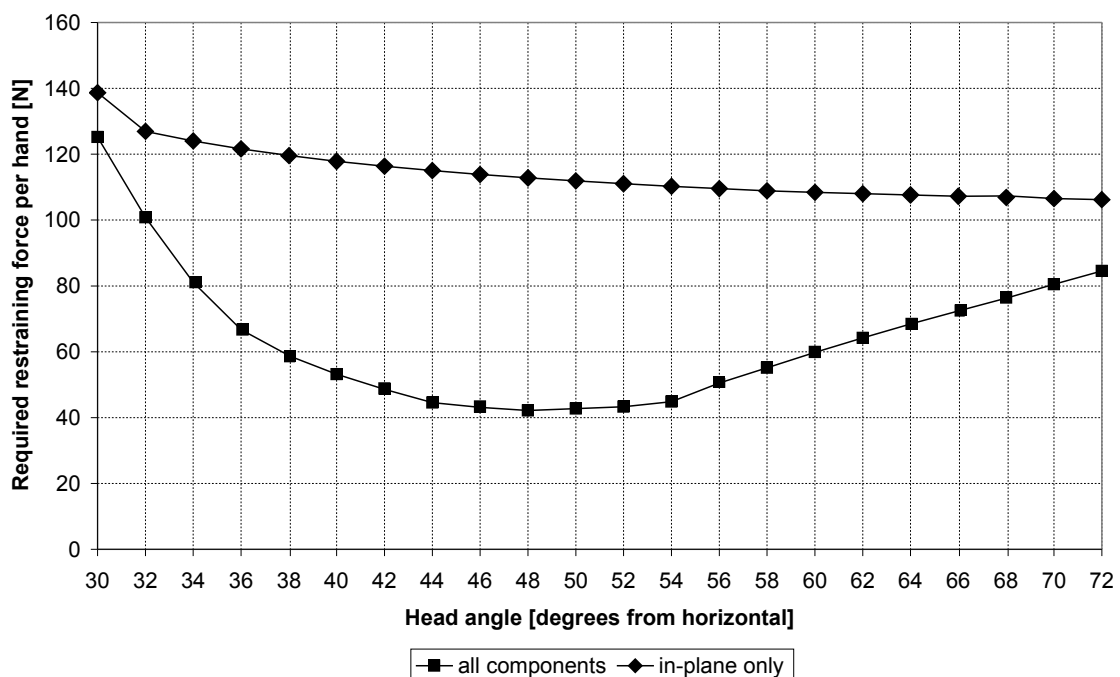


Figure 15: Peak restraining force per hand vs. head angle

The “in-plane only” curve of figure 15 shows no benefit at all in inclining the head axis, in fact there is a slight drawback. This is because, as the head angle decreases, the mechanical advantage of the hands is diminishing at a faster rate than that of the pedal forces. When all the components are included, there is still a benefit in lower head angles. The improvement comes from the greater lever arm gained by the out-of-plane forces due to the greater fork offset at shallower head angles. However, as shown in the figure, there is little point in inclining the head angle below 54 degrees. It should be remembered that this model of hand restraint assumes that the hands restrain only the forces that are aligned with the rider’s outstretched arms (as depicted in figure 5). In reality there will be some restraint by the arms in other directions, for example in the plane of rotation of the handlebars. However, the mechanical advantage of the arms in these other directions is comparatively weak, so figure 15 gives a good indication of the restraining effort required of the rider in the over-seat steering, arms outstretched position.

Figure 16 depicts the peak restraining force per hand expressed as a percentage of the peak pedal force. This figure shows that the peak restraining force per hand can be as low as 13% of the peak applied pedal force. This underscores that riding a direct-drive recumbent is not a tug-of-

war between the rider's legs and arms—the force transmitted back to each hand is about an order of magnitude less than that applied to the pedals.

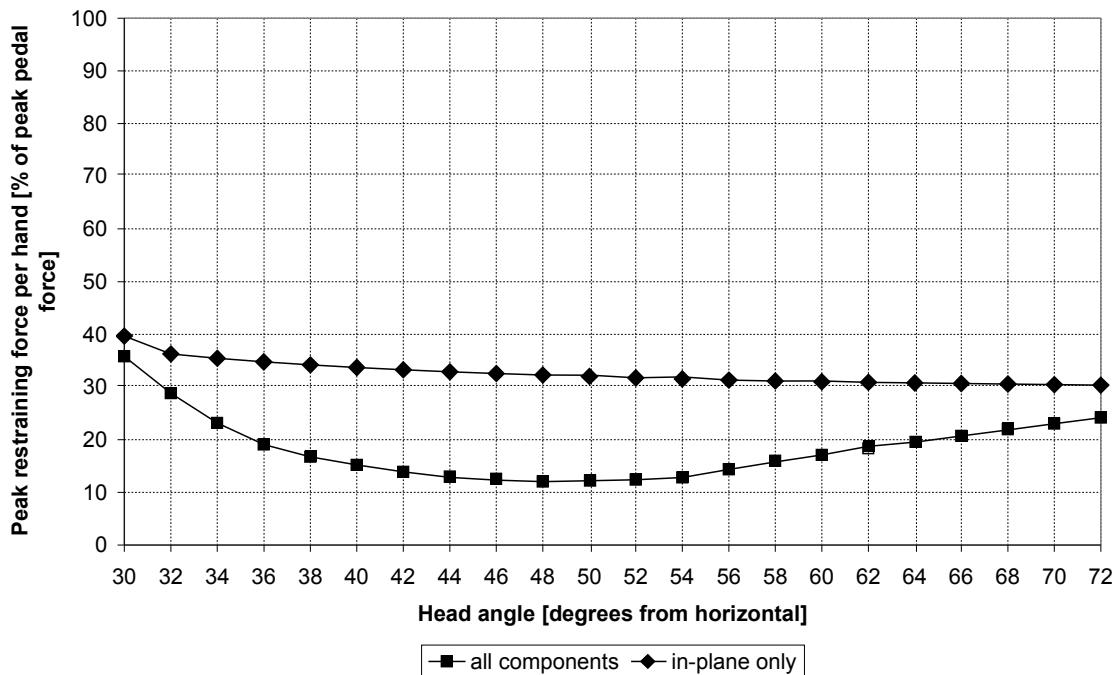


Figure 16: Peak restraining force per hand as a percentage of peak pedal force

### Reducing the head angle vs. increasing seat height

Increasing the seat height will reduce the pedal force feedback by the same principle as inclining the steering axis (i.e. by aligning the pedal forces more closely with the steering axis). Of course at the limit the seat height will no longer be recumbent, but it is nonetheless instructive to see the effect of a small seat height increase on the pedal force feedback. Figure 17 depicts the effect of a seat height increase versus a decrease in head angle. The initial seat height is that of the variable geometry bike (554 mm) and the initial head angle is taken as 62 degrees to the horizontal (the same as the author's direct-drive bike shown in figure 1). The peak handlebar restraining force is the benchmark, rather than the torque about the steering axis, and the same plane of restraint (14 degrees from the horizontal) is assumed for all seat heights (in reality there might be some increase in this angle with higher seat heights).

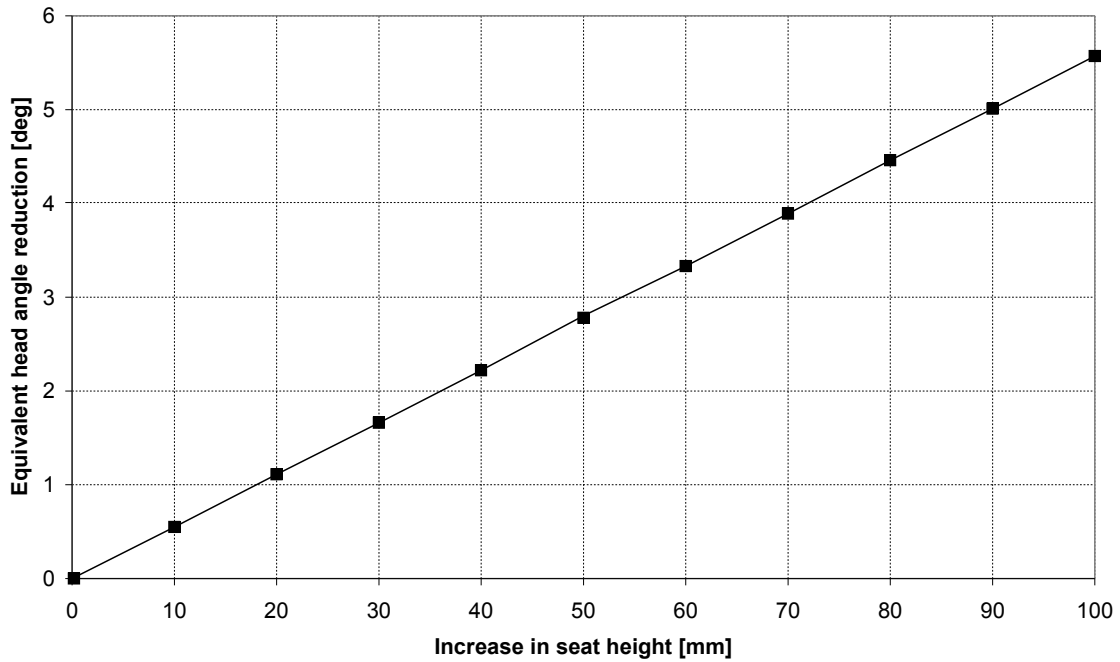


Figure 17: Head angle vs. seat height

Figure 17 indicates that raising the seat 50 mm will reduce the peak handlebar restraining force by the same amount as reducing head angle by about 3 degrees. Although a head angle of 62 degrees was used as a benchmark, there will be a similar effect at other head angles since the slope in figure 15 is fairly constant from 54 degrees upward. Therefore a higher seat can have a similar effect to reducing the head angle, and without the handling problems associated with shallower head angles.

### Reducing the head angle vs. increasing handlebar width

Similarly, an increase in handlebar width will reduce the force to the hands. Figure 18 shows the effect of a handlebar width increase versus a decrease in head angle. The initial handlebar width is that of the variable geometry frame (465 mm between the centre of each handlebar grip), and the initial head angle 62 degrees.

An increase in overall handlebar width by 50 mm is equivalent to a head angle reduction of about 3 degrees, as shown in figure 18. This is a worthwhile improvement, but as with seat height there are limitations. Handlebars that are too wide can cause difficulty when passing through narrow spaces and in the storage and parking of the bike. The arms must also move through a larger distance for the same steering angle, so the steering feels slower. Of course, some reduction gearing or linkage in the steering would give a similar reduction in force feedback without the extra width, but this would still slow the steering response and unwanted complexity would be added. Therefore a small increase in handlebar grip width is judged advantageous.

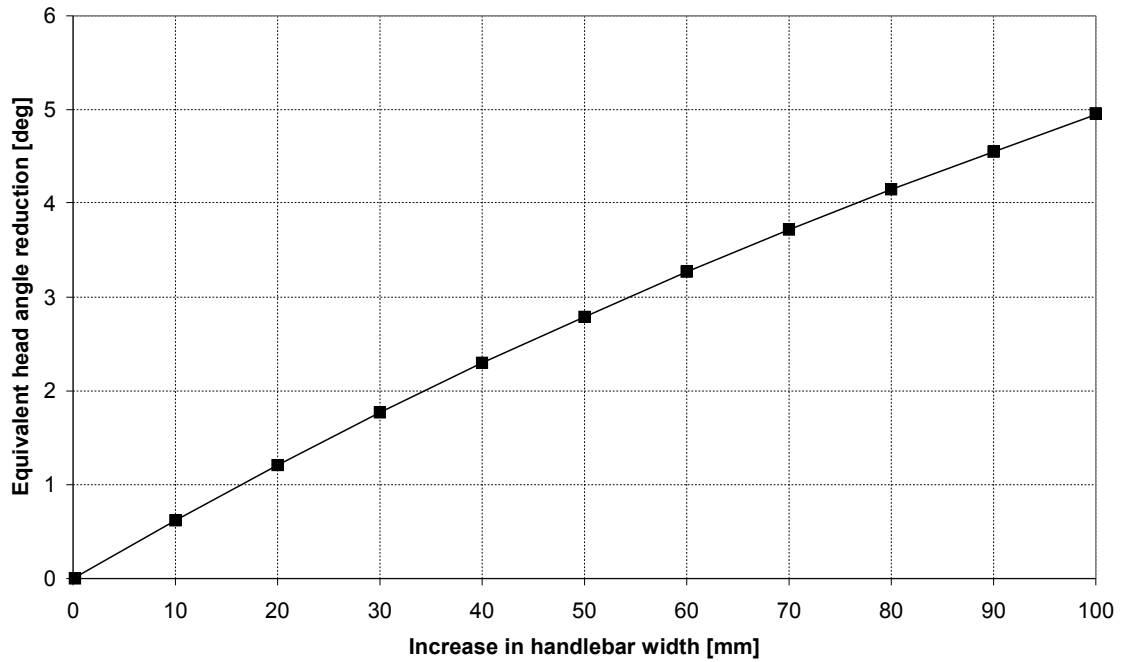


Figure 18: Head angle vs. handlebar width

### Reducing the head angle vs. reducing the tread

The tread, defined here as in table 1<sup>7</sup>, also has an effect on the pedal force feedback. Figure 19 depicts a decrease in tread versus a reduction in head angle. The initial tread is taken as that of the variable geometry frame (297 mm lateral distance between the centre of each pedal), and the initial head angle 62 degrees.

The force feedback is more than doubly sensitive to a reduction in tread than it is to either a seat height increase or a handlebar width increase. As illustrated in figure 19, reducing the tread by a mere 20 mm is equivalent to a head angle reduction of more than three degrees. However the effect may not be quite this extreme due to higher outward lateral pedal forces as the tread increases.

<sup>7</sup> Strictly speaking the tread is the lateral distance between the outer surfaces of the cranks, rather than as defined in table 1. The tread is also known as the Q-factor.

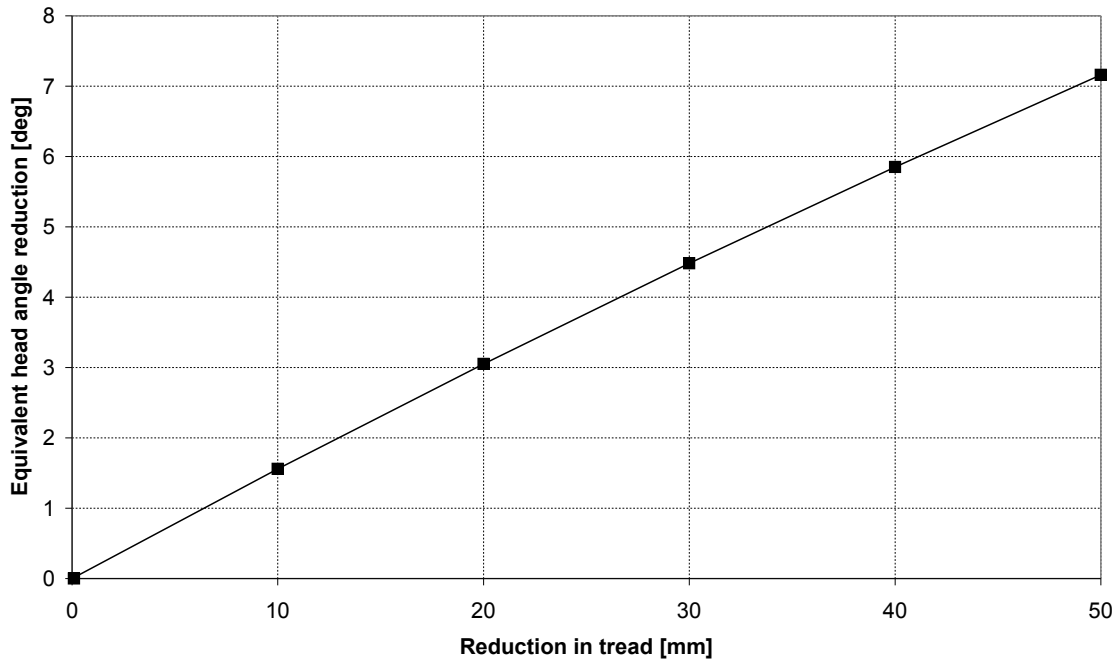


Figure 19: Head angle vs. tread

### Comparing to other moving bottom bracket (MBB) bikes

It is instructive to compare the direct-drive recumbent with other recumbent bikes with moving bottom brackets (MBB). These other designs usually have a bottom bracket mounted generally above and in front of the front wheel, with a chain extending back to a front hub or derailleur gear. Examples are the Flevobike, Cruzbike™, Python (see Openbike (2008)), and bicycles developed by Tom Traylor (see for example United States design patent D277,744). Compared to a direct-drive recumbent, the steering axis is much further behind the pedals and thus the lateral outward pedal forces have a greater leverage around the steering axis, leading to reduced pedal force feedback. The distance from the steering axis to the bottom bracket can be in the range of 40-50 cm.

Figure 20 compares the pedal force feedback of two chain-driven MBB bikes with that of the direct-drive recumbent. The first chain-driven MBB bike is typical of a full size wheel (700C) configuration, with a steering axis to the bottom bracket distance of 47 cm. The large front wheel dictates a high bottom bracket and thus a recumbent angle of 73 degrees is typical (bottom bracket at hip pivot height). The second chain-driven MBB bike is typical of the small front wheel design, with a low bottom bracket giving a recumbent angle of 53 degrees and a steering axis to the bottom bracket distance of 40 cm. An above seat handlebar position similar to that of the direct-drive recumbent is assumed for both designs.

Comparing the curves in figure 20, a chain-driven MBB bike has a considerably lower restraining force than a direct-drive recumbent, except in the very shallow head angle range where the poor leverage in the plane of the outstretched arms overrules. For the large wheel design the minimum is 34% of the direct-drive minimum, and this reduces to 31% for the small wheel configuration. The minimum head angle for the small-wheel design also comes at more convenient head angle of 66 degrees, versus the 52 degree for the large-wheel case. Both chain-driven bikes show considerably lower pedal force feedback than direct-drive for the full extend



of practical head angles (56-72 degrees), however, and with less increase with increasing head angle in this range.

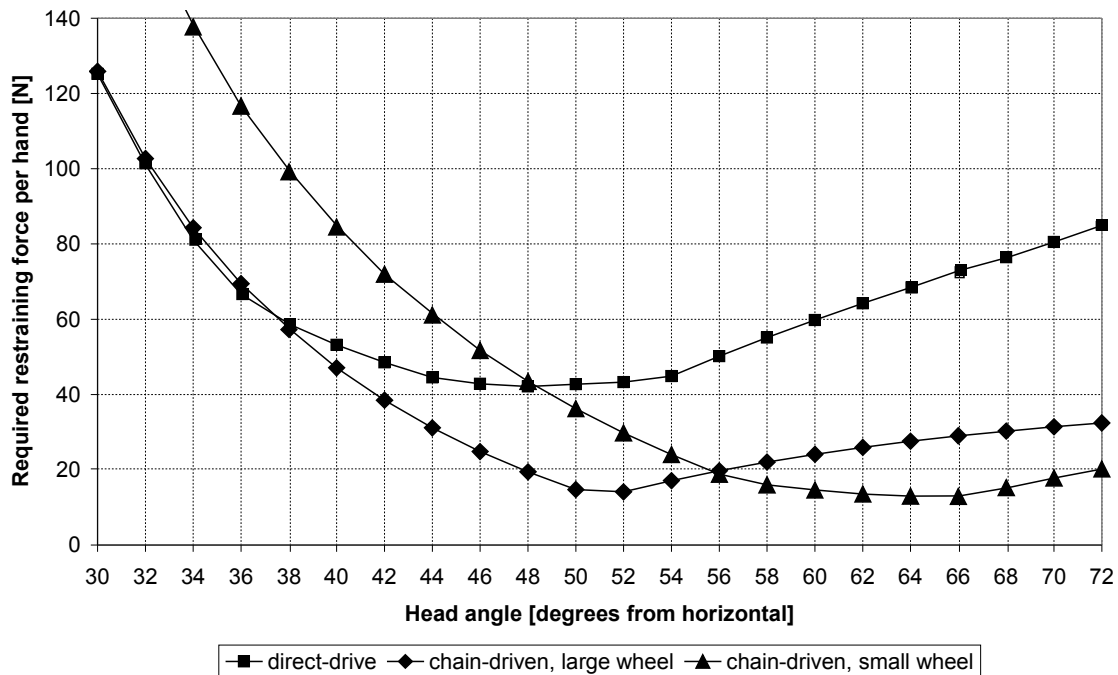


Figure 20: Direct-drive compared to chain-driven MBB bikes

This underscores the important role of the leverage of the out-of-plane forces in reducing the pedal force feedback—and illustrates the particular challenge facing the direct-drive recumbent designer, whose lever arm is limited to the available fork offset.

## B. HANDLING ANALYSIS

### Trail as a function of head angle

Figure 21 shows trail as a function of head angle as calculated using equation 18. As can be seen, the trail of the front wheel varies very little in the head angle range of interest (52 to 62 degrees). This figure also agrees with the 2-3 cm proposed by Kretschmer (2000) for shallow head angles.

### Centering spring constant vs head angle

Figure 22 depicts the spring constant for the centering spring as a function of head angle, as calculated using equation 23.

The centering spring rate increases rapidly with decreasing head angle, reflecting both the increasing fork offset and the increasing mechanical advantage of the applied forces. For example, the spring rate required for a 50 degree head angle is double that of a 62 degree head angle. This illustrates the importance of a centering spring as the head angle gets shallower.

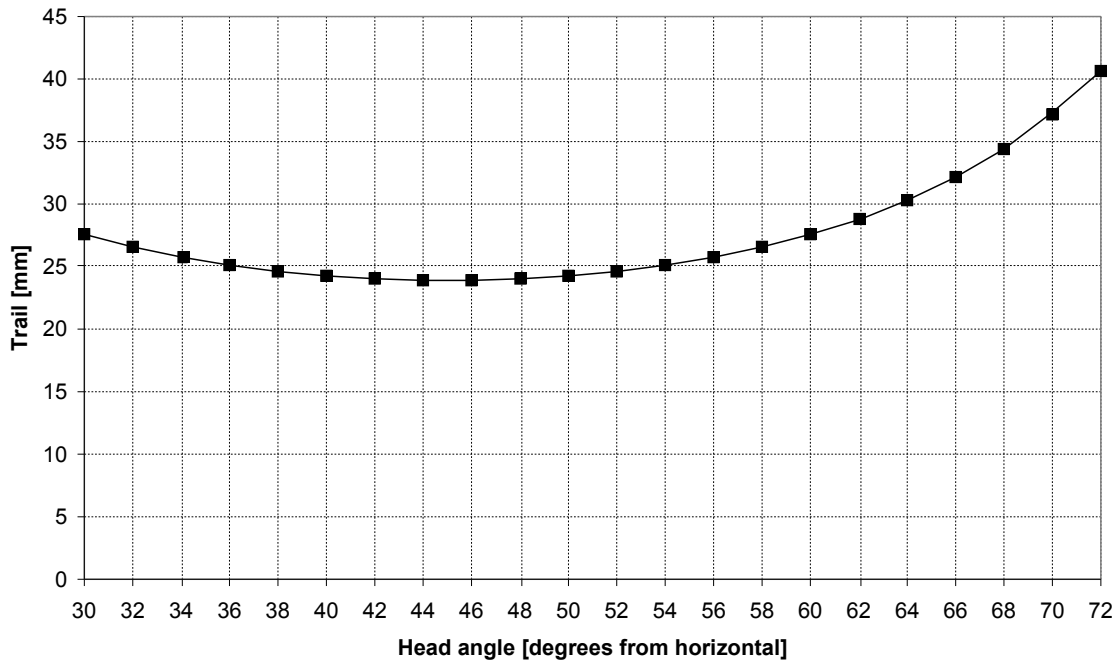


Figure 21: Trail vs. head angle

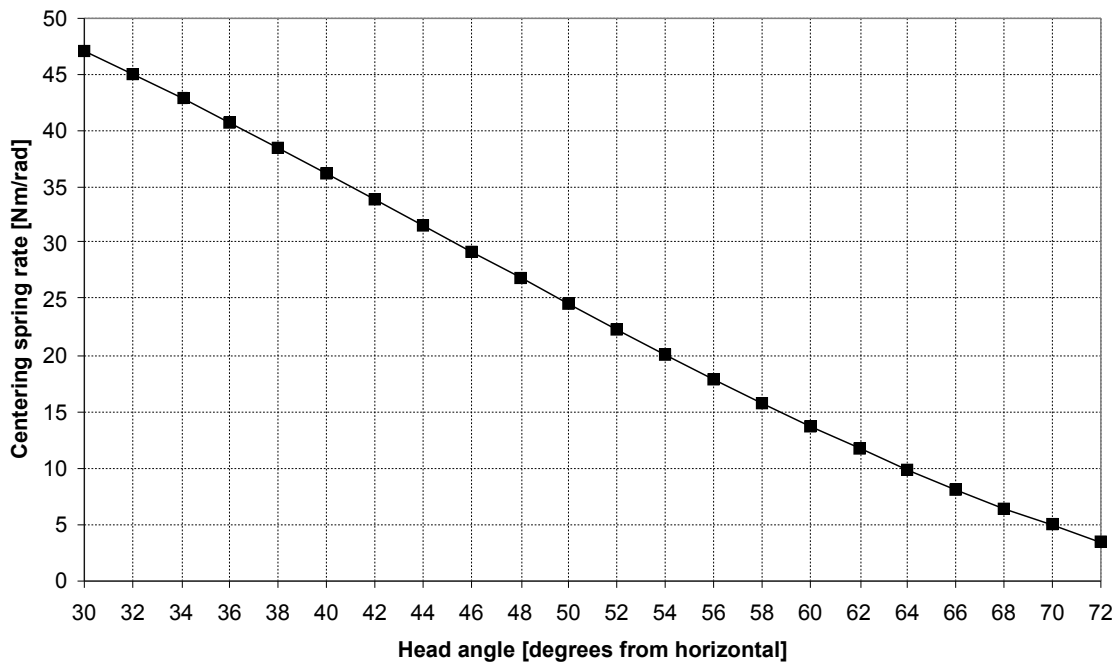


Figure 22: Spring rate vs. head angle

### C. EXPERIMENTAL ANALYSIS

The results of the test runs are of necessity somewhat subjective. The rider is the author in each case. The scope is to give a qualitative assessment and to look for practical aspects of the rider/bike interface. The goal is to define the best compromise between low pedal force feedback and good handling. The test runs are done using the variable geometry bike (figure 10) with a front wheel trail calculated by equation 18 and, except as noted, a centering spring designed according to equation 23. The author's direct-drive bike (figure 1) is included for comparison, and it has a front wheel trail of 28.6 mm (1.125 in) and no centering spring. For all the tests, the rider's feet were not constrained by clips or cleats.

**62 degree head angle (author's bike of figure 1):** Although the force feedback is quite manageable, it requires a secure grip on the handlebars most of the time. One-handed riding can be done when coasting, or when pedaling gently provided that the hand is held very securely. High speed stability and tracking is good, but coasting hands-free is virtually impossible, with the bike over-controlling (turning more into the fall than required). A shift in crank position when coasting causes some instability, requiring one to increase the grip a little. One can sense a slight torque on the steering when coasting which varies as one changes pedal position. Low speed tracking is excellent allowing the bike to be ridden with confidence at walking speed, and in narrow areas, but sudden increases in pedal force require an anticipated resistance from the arms to keep the bike on the desired track.

**58 degree head angle:** The force feedback is only slightly less than the 62 degree case, requiring a good grip on the handlebars when pedaling under steady load. Low speed tracking is very good, but no better than the 56 degree case. As with the 62 degree case, some concentration is required to anticipate the necessary increase in restraining force to keep the bike on track when the pedal force is increased. Hands-free coasting is slightly better than the 56 degree case, with the bike over-controlling slightly. Riding with one hand on the handlebars is possible, but it requires a firm grip under moderate pedal load.

**56 degree head angle:** The force feedback is noticeably less than the 62 degree case: the bike could be pedaled with a moderate grip on the handlebars when cruising steadily and with only one hand on the handlebars when pedaling gently. However a firm grip is needed on both handlebar grips when pedaling hard. Low speed tracking is very good though not quite as good as 62 degrees, but the bike can still be ridden with confidence on multi-use paths with pedestrians. High speed tracking and stability is noticeably better than the 62 degree case, with brief periods of hands free coasting possible, but not advisable. When coasting hands-free, the bike appears to under-control a little, requiring a quick application of a hand to the handlebars to turn sharper into the fall. A change in crank position while coasting causes some instability when coasting hand-free, and usually requires an application of the hands to the bars to recover. However, the level of disturbance from a change of crank position is less pronounced than the 62 degree case.

**54 degree head angle:** The force required to restrain the steering is not perceptively less than for the 56 degrees case. However, the low speed tracking confidence is considerably worse, and one cannot ride so close to walls and posts with the same degree of assurance. Hands-free coasting is slightly better than 56 degrees allowing longer hands-free runs, but the bike eventually over-controls slightly, needing a restoring turn to the steering. The stiffer centering spring than the 56 degree case made the bike more difficult to maneuver when walking it. When coasting, the response to a change in crank position is similar to that of the 56 degree case.

**52 degree head angle:** Pedal force feedback is noticeably less than the 54 degree case, but the

movement of the steering feels less intuitive for the outstretched position of the arms. The arm's natural fore and aft direction of movement does not correspond well with the handlebar's movement which is more side to side. The front assembly is considerably more unwieldy than with the 54 degree case and the steering noticeably slower to respond. Tracking is therefore less precise and riding with pedestrians and in tight constraints is approached with some trepidation. Hands-free coasting is possible but a slight lean causes the bike to over-control.

**50 degree head angle:** Tracking is less precise than the 52 degree case, and riding in narrow areas or with pedestrians requires a lot of concentration to prevent large unwanted swerves. The bike has more of a "hinge-in-the-middle" feel and one can sense the frame of the bike squirming slightly under the seat when steering. Pedal force feedback is low, but the counterintuitive motion of the handlebars relative to the hands is more evident than with the 52 degree case. Hands-free coasting is quite good but the bike ultimately over-controls.

**54 degree head angle, stiffer centering spring:** This is to test the effect of a stiffer spring than that calculated using equation 23. To do this the spring for the 52 degree case is used with the 54 degree head angle. Low speed tracking is improved over the regular spring, but it is still not as good as the 56 degree case. Hands-free coasting is also better than with the regular spring. However, initially the steering response feels a little unusual causing some unease. This diminished quickly with riding. Overall, there is an improvement over the regular spring.

## DISCUSSION

Figure 23 presents a convenient way of visualizing the pedal force feedback results. As shown in the figure, the rider exerts a pedal force extending in an outward-V from the centre of pressure of the rider on the seat to the pedals. The angle of this V produces the outward lateral pedal forces. Clearly, the closer the steering axis is to the rider's centre of pressure, the lower the resulting pedal force feedback. This is due the correspondingly smaller lever arm around the steering axis as the steering axis approaches the vertex of the V. Thus the goal of the designer is to minimize the distance L in figure 23. This is consistent with Openbike (2008), who imply that in order to avoid any pedal force feedback, the steering axis should be aligned between the rider's hip pivots. As can readily be seen, the distance L in figure 23 can be minimized by any of three ways: a) moving the steering axis further back (i.e. decreasing the trail); b) decreasing the head angle; and c) increasing the seat height.

Unlike other moving bottom bracket bikes such as the Flevobike, the direct-drive recumbent designer does not have the luxury of translating the steering axis back toward the seat to reduce pedal force feedback—this would produce too much negative trail. Instead the designer is left with the remaining approaches: decreasing the head angle, increasing the seat height, increasing the handlebar width and reducing the tread. So the practical limits to these adjustments are critical to the design.

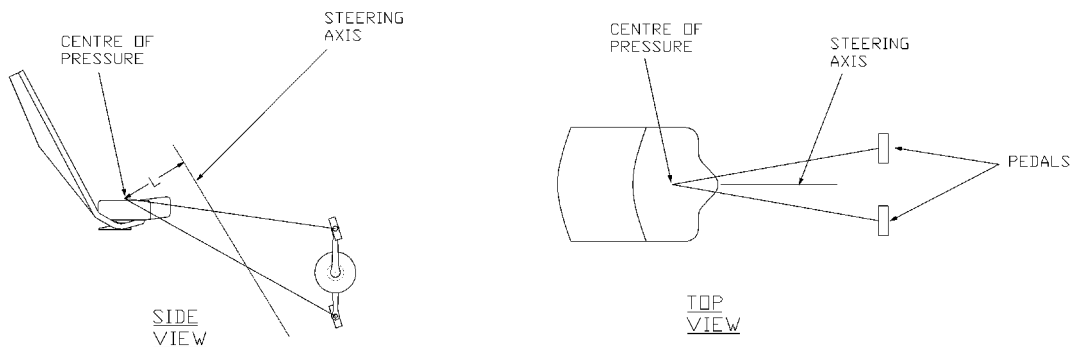


Figure 23: Pedal force path visualization

### Minimum head angle

From the test runs, it is clear that a head angle of 56 degrees represents the minimum practical limit for user-friendly riding. Further reduction slows the steering response and causes a handlebar motion that is inconsistent with the plane of the outstretched arms of the rider.

### Maximum seat height

The maximum seat height is determined by two criteria a) the rider's feet must still be comfortably placed on the ground without too much compression of the seat cushion by the rider's legs, and b) the centre of mass of the bicycle and rider must remain low enough to avoid pitch-over in emergency braking.

From the author's own riding experience, a compressed seat height of 56 cm ensures that the rider's feet can be placed on the ground without discomfort. Given the author's size (1.83 m tall, 0.841 m hip pivot to bottom bracket), this seat height corresponds to a recumbent angle of 53 degrees, where the compressed seat height is defined as 76 mm below the rider's hip pivot

Calculations indicate that a seat height of 56 cm would not produce any pitch-over in emergency braking. This is based on the centre of mass of the bike and rider (determined experimentally) and an assumed maximum tire friction factor of 0.8<sup>8</sup>.

Therefore a recumbent angle of 53 degrees is considered to be a good compromise between rider comfort/safety and reduced pedal force feedback.

### Maximum handlebar width

<sup>8</sup> A friction factor of 0.8 is at the upper end of a typical range for a bicycle tire (Wilson (2004), p.245).

The author's direct-drive recumbent and the variable geometry bike both have a handlebar width of 465 mm between the handlebar grip centers. Given an inverted U or W handlebar design, this width could be increased to 560 mm without being unduly cumbersome. The inverted U or W shape allows the center of pressure of the hands to be further apart for a given overall width, and provides greater knee clearance.

### Minimum tread

The tread value of 297 mm (centre-of pedal to centre-of-pedal) used in the calculations and on the variable geometry bike is approaching the practical limit of narrowness. The front hub of the test bike is based on an adaptation of a commercially available planetary chain ring unit (Schlumpf Speed-Drive®), so the tread is similar to that of a regular upright bike with a standard 68 mm wide bottom bracket. It is not really practical to reduce the tread to less than 297 mm.

### Other design issues

For a regular upright bicycle, the rigidity of the frame is essential for efficient pedaling. For a direct-drive recumbent the equivalent concern is the rigidity of the front assembly, particularly the rigidity in torsion from the front wheel to the handlebars. Therefore, instead of the conventional fork design where the steerer tube passes through the head tube of the frame, the fork should lead directly from the front wheel to the handlebars with the connection to the head offset behind the fork. In this way there is no narrowing required to pass through the head tube, and the rigidity in torsion is improved.

Kretschmer (2000) suggests a wheelbase of 1200 mm for a direct-drive recumbent, and Stegmann (2002) presents a wheelbase of 1450 mm. The author's direct-drive recumbent has a wheelbase of 1524 mm, and the variable geometry bike has a wheelbase of 1475 mm. While there is the space for a wheelbase as short as the 1200 mm proposed by Kretschmer, there may be traction problems on hills due to the lightly loaded front wheel. The wheelbase should set to achieve a 50/50 weight distribution, for traction and ride quality. For most riders, this will result in a wheelbase ranging from 1300 mm to 1550 mm.

## CONCLUSION—RECOMMENDED DESIGN

Table 3 presents the recommended design parameters for a user friendly direct-drive recumbent, based on the results of this study.

Table 3: Recommended design

Wheel size	700C front and rear
Wheelbase	1300 to 1550 mm (51 to 61 inches)
Head angle	56 degrees from the horizontal
Centering spring rate	based on equation 23, then adjusted for particular rider
Trail of the front wheel	25 mm (1 inch)
Seat height	560 mm (22 inches) for 1.83 m rider
Recumbent angle	53 degrees
Tread	297 mm (11.7 inches) between pedal centers
Handlebar position	over-seat, arms outstretched
Handlebar type	inverted-U or inverted-W
Handlebar width	560 mm (22 inches) between handlebar grip centers

This design returns only 12 % of the peak applied pedal force to each hand of the rider.

The resulting bicycle is shown in Figure 24. The fork extends continuously from the front wheel to an integral steerer tube, to which the inverted-U handlebars are attached. An intermediate tube connecting the fork to the head tube is attached behind the fork, and located at the lowest possible location on the fork to ease step-over. Both the fork and head tube are inclined at 56 degrees to provide a simplified perpendicular attachment for the intermediate tube. The axis of the head tube intersects the ground 25 mm ahead of the front wheel contact point, giving a trail of 25 mm. On the other side of the head tube, the frame follows in the same direction of the intermediate tube until the bend upward for the seat support section of the frame. The height of the seat above the seat support section is set for a recumbent angle of 53 degrees. The seat section slopes up at 20 degrees to give a consistent recumbent angle of 53 degree, regardless of seat position on the tube. Approaching the rear wheel, the frame splits into the rear fork and slopes down to the rear wheel dropouts. The head tube contains a torsion bar which is easily exchangeable to give a spring rate adjustment.

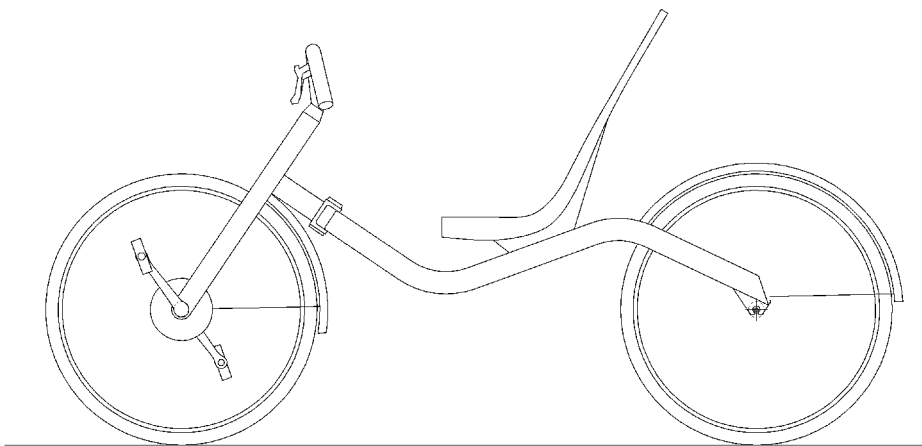


Figure 24: Recommended design

## REFERENCES

Davis, R. R., and M. L. Hull (1981). "Measurement of pedal loading in bicycling: II. Analysis and results." *Journal of Biomechanics* 14:857-872.

Fehlau, Gunner. (2003). *The Recumbent Bicycle*, 2nd ed. Grand Rapids: Out Your Backdoor Press.

Garnet, Jeremy. (2003). "Delving into direct drive." *Velo Vision*, no. 12:18-20 (December).

Hull, M. L., and R. R. Davis (1981). "Measurement of pedal loading in bicycling: I. Instrumentation." *Journal of Biomchanics* 14:843-855.

Kretschmer, Thomas (2000). "Direct-drive (chainless) bicycles.", *Human Power*, no. 49:11-14.

Openbike (2008) [http://en.openbike.org/wiki/Pedal/Steering\\_Interference](http://en.openbike.org/wiki/Pedal/Steering_Interference).

Papadopoulos, Jim. (1987). "Bicycle steering dynamics and self-stability: A summary report of work in process." Cornell Bicycle Project report, December 15; <[http://ruina.tam.cornell.edu/research/topics/bicycle\\_mechanics/papers/bicycle\\_steering.pdf](http://ruina.tam.cornell.edu/research/topics/bicycle_mechanics/papers/bicycle_steering.pdf)>

Stegmann, John. (2002). "Chain of thought." *Velo Vision*, no. 8:22-25 (December).

Wilson, David Gordon. (2004). *Bicycle Science*, 3rd ed. Cambridge, Massachusetts: The MIT Press.